

Zeitschrift: IABSE reports = Rapports AIPC = IVBH Berichte
Band: 999 (1997)

Artikel: CFT beam-column connection with high strength materials
Autor: Fukumoto, Toshiyuki / Sawamoto, Yoshikazu
DOI: <https://doi.org/10.5169/seals-1012>

Nutzungsbedingungen

Die ETH-Bibliothek ist die Anbieterin der digitalisierten Zeitschriften. Sie besitzt keine Urheberrechte an den Zeitschriften und ist nicht verantwortlich für deren Inhalte. Die Rechte liegen in der Regel bei den Herausgebern beziehungsweise den externen Rechteinhabern. [Siehe Rechtliche Hinweise.](#)

Conditions d'utilisation

L'ETH Library est le fournisseur des revues numérisées. Elle ne détient aucun droit d'auteur sur les revues et n'est pas responsable de leur contenu. En règle générale, les droits sont détenus par les éditeurs ou les détenteurs de droits externes. [Voir Informations légales.](#)

Terms of use

The ETH Library is the provider of the digitised journals. It does not own any copyrights to the journals and is not responsible for their content. The rights usually lie with the publishers or the external rights holders. [See Legal notice.](#)

Download PDF: 20.05.2025

ETH-Bibliothek Zürich, E-Periodica, <https://www.e-periodica.ch>

CFT Beam-Column Connection with High Strength Materials

Toshiyuki FUKUMOTO

Senior Research Eng.
Kajima Corp.
Tokyo, Japan

Toshiyuki Fukumoto, born 1956, graduated from Tokyo Denki Univ. His main research interests are composite structures, recently concrete filled steel tube structures.

Yoshikazu SAWAMOTO

Research Eng.
Kajima Corp.
Tokyo, Japan

Yoshikazu Sawamoto, born 1965, received Master degree of Eng. from Kyoto Univ. His main research interests are composite structures and connection of steel structures.

Summary

This study examined two types of CFT beam-column connections which employed high strength steel (590, 780MPa) and high strength concrete (60-120MPa). The connections have less difficulties in filling the concrete mixture in column steel tubes. One type has inner diaphragm with large opening, and the other type has external vertical stiffeners. This study employed structural tests for clarifying the structural characteristics of these connections and for developing a prediction method of ultimate load resistance of these connections.

1 Introduction

Concrete Filled steel Tube (CFT) Columns are expected high load resistance by using high strength concrete and high strength steel, and this high resistance extends to the practical application of these CFT columns to large structures such as high rise buildings. High performance building structures using these CFT columns, which employed high strength steel (590, 780MPa) and high strength concrete (60-120MPa), and steel beams have been under development by the authors. However, these structures have difficulties in filling concrete into the column steel tubes since fresh mixture of the high strength concrete is very viscous. This difficulty is aimed at being overcome by using new types of beam-column connections, which are: 1) with diaphragm having wide opening and large thickness, or 2) with vertical stiffeners outside of a column steel tube, which are installed between beam flanges to avoid interference with finishing material and reinforcement in floor slab (Fig. 1).

Similar connections have been investigated by Morita et al, but have different geometry from those connections presented herein. Furthermore, few researches have done by examining the connections with high strength constitutive materials. Therefore, the authors conducted local tension tests and shear test for the connection to clarify the elasto-plastic behavior of the connections. Moreover, a methodology for predicting load resistance of the connection is also investigated in this study.

2 Outline of Tests

The local tensile test and the shear test on the proposed beam-column connections are conducted. The specimens' geometry is classified into two types, one with diaphragm having opening (ID type) and the other with vertical stiffeners (VS type) as shown in Fig. 2 and Fig. 3, and the parameters of specimen are summarized in Tables 1, 2 and 3.

As shown in Table 1, tensile tests for ID type involve six specimens, in which experimental parameters are: diaphragm thickness, opening shape in diaphragm, width-thickness ratio of steel tube, beam-column width ratio (B/D , see Fig. 2) and steel strength. Tensile tests for VS type also comprise six

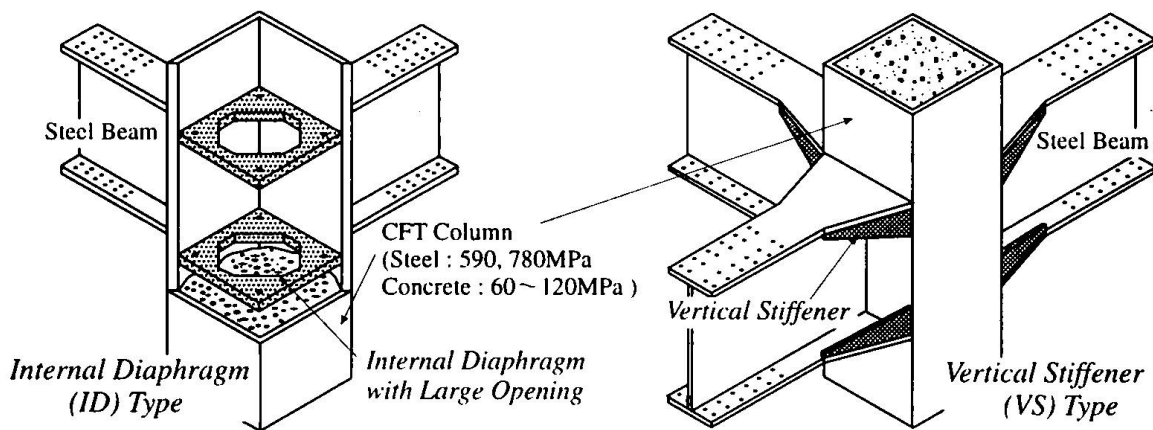


Fig. 1 Outline of Beam-Column Connection

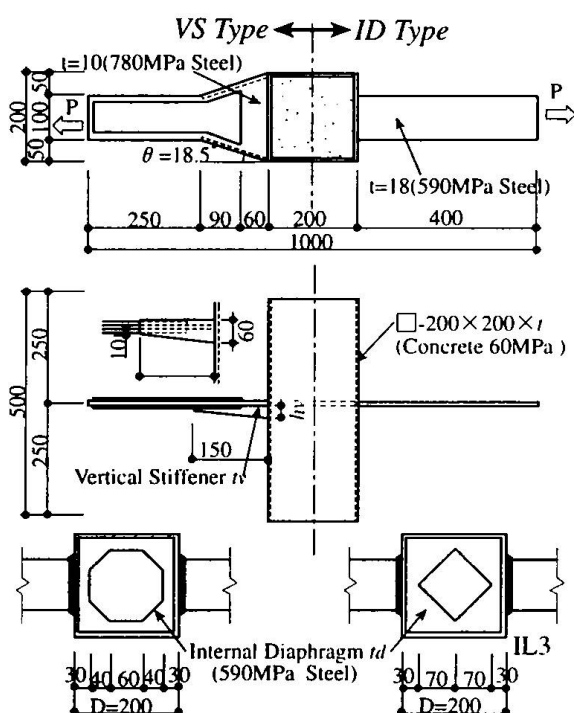
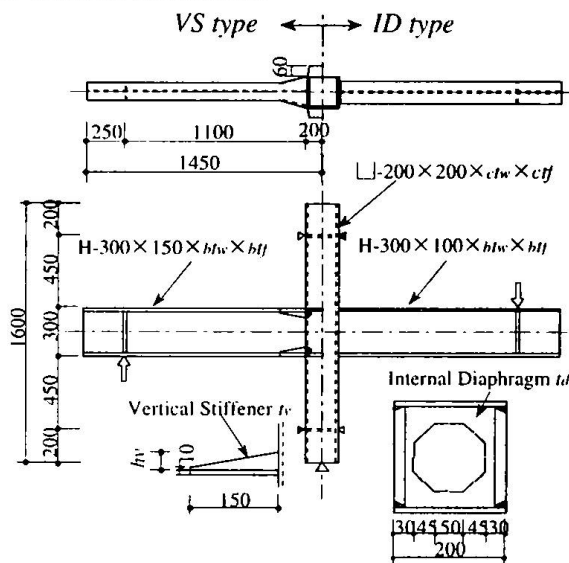


Fig. 2 Specimens of Tensile Tests



Stiffening Type	ID type			VS type		
Specimens	IP1	IP2	IP3	VP1	VP2	VP3
ctw	6	9	8	6	6	8
ctf	9	12	12	9	9	12
btw	9	12	12	12	12	14
btf	14	14	14	19	19	25

unit: mm

Fig. 3 Specimens of Subassembly Tests

specimens, in which experimental parameters are: stiffener height, stiffener thickness, width-thickness ratio of steel tube, and steel strength (Table 2).

Shear tests incorporate six specimens in which three specimens are ID type and the other three are VS type. Experimental parameters are steel tube's width-thickness ratio for ID type and connection panel's height-width ratio for VS type. Furthermore, steel strength and concrete strength are changed as parameters for both types of specimens. These shear tests employ common condition other than those indicated in experimental parameters (Table 3). The above tests adopted two classes of steel tube's width-thickness ratios, FA class and FC class. Steel tubes of FA class are commonly used in Japanese industry, and those of FC class have 1.5 times higher thickness-width ratio than FA class. These FC class tubes are permitted for use particularly to CFT columns while not being commonly used in the construction industry due to the vulnerability of buckling.

Tensile test specimens are rectangular CFT columns with single beam flanges, and tensile loads are applied to the ends of flange plates, as shown in Fig. 2. Shear test specimens are beam-column connections which are assumed as subassemblies composing entire frame as shown in Fig. 3. The shear force is applied to the connections through beam flanges as in this figure. Both tensile

Table 1 Specimens for Tensile Test of ID Type

Specimens		IL1	IL2	IL3	IL4	IL5	IL6
Diaphragm	Opening Shape ¹⁾	O	O	Q	O	O	O
	Thickness t_d (mm)	9	14	9	9	9	9
Width-Thickness Ratio D/t (class) ²⁾		33(FC)	33(FC)	33(FC)	33(FC)	22(FA)	29(FC)
Strength of Steel (MPa)		590	590	590	590	590	780
Beam-Column Width Ratio B/D		1/2	1/2	1/2	1/3	1/2	1/2

Note 1) : O:Octago, Q:Quadrangle

2) : D :Depth of steel tube, t :Thickness of steel tube

Table 2 Specimens for Tensile Test of VS Type

Specimens		VL1	VL2	VL3	VL4	VL5	VL6
Stiffener	Height h_v (mm)	6	6	6	14	9	7
	Thickness t_v (mm)	30	50	50	30	30	30
Width-Thickness Ratio D/t (class) ²⁾		33(FC)	33(FC)	33(FC)	33(FC)	22(FA)	29(FC)
Strength of Steel (MPa)		590	590	590	590	590	780

Note 1) : D :Depth of steel tube, t :Thickness of steel tube

Table 4 Properties of Steel

Steel (MPa)	Thickness (mm)	σ_y (MPa)	σ_u (MPa)
590	5.6	533	689
	5.9*	514	653
	8.4	527	691
	8.9*	511	654
	13.4	572	716
780	7	836	859
	8.0*	796	854
	10	841	869

 σ_y : Yield point σ_u : Tensile strength

* : Shear tests

Table 4 Properties of Concrete

Test	σ_c (MPa)
Tensile test	57.7
Shear test	64
	116.9

 σ_c : Compressive strength

Table 3 Specimens for Shear Test

Stiffening Type	ID type			VS type		
Specimens	IP1	IP2	IP3	VP1	VP2	VP3
Width-Thickness Ratio D/t (class) ¹⁾	33(FC)	22(FA)	25(FC)	33(FC)	33(FC)	25(FC)
Strength of Steel (MPa)	590	590	780	590	590	780
Strength of Concrete (MPa)	60	60	120	60	60	120
Height-Width Ratio	1.5	1.5	1.5	1.5	1.0	1.5

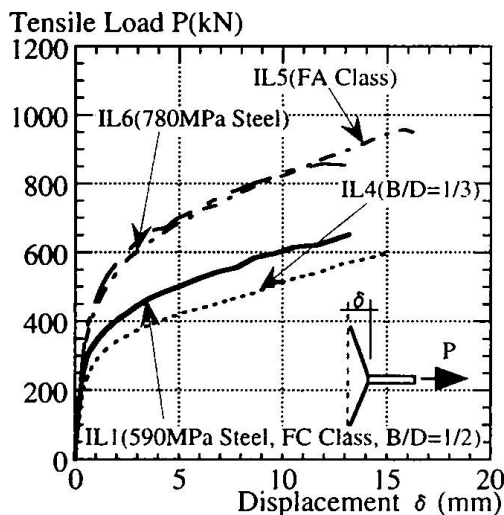
Note 1) : D :Depth of steel tube, t :Thickness of steel tube

Fig. 4 Tensile Tests Result on ID Type

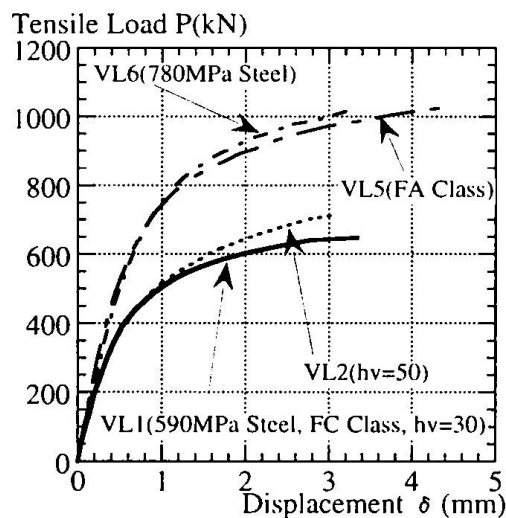


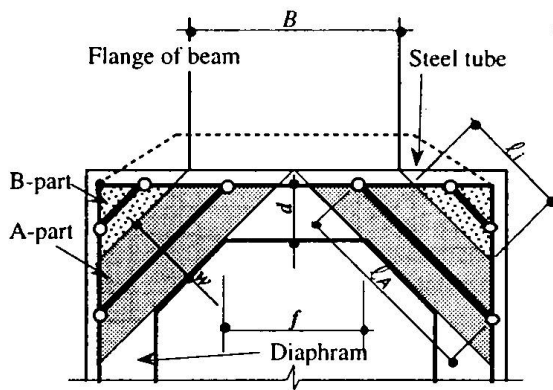
Fig. 5 Tensile Tests Result on VS Type

and shear loading are applied in monotonic manner.

3 Structural Characteristics of Local Parts of the Connections

3.1 Test Results

Tensile test results for ID type are illustrated in Fig. 4, in which load-displacement relationships are summarized. ID type specimens showed failure by crack propagation in the steel tube flange to



$$P_u = P_c + P_d$$

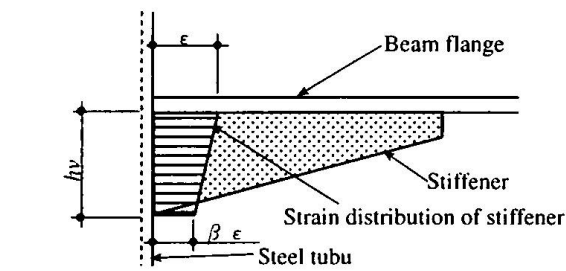
$$P_d = \frac{2}{\sqrt{2}} \left(W + \frac{\ell_i}{4} \right) t_d \cdot \sigma_{du}$$

$$W = \min \left(w, \sqrt{2} \frac{B}{2} \right) \quad w = \frac{1}{2\sqrt{2}} (B - f + 2d)$$

$$\ell_A = \min \left(\ell_i + W, \ell_i + \sqrt{2} \frac{B}{2} \right) \quad \ell_i = \frac{1}{\sqrt{2}} (D - B - 4t)$$

P_c : Morita's yield line theory for ultimate out-of-plane resistance of steel tube's flange⁽¹⁾
 t : Thickness of steel tube
 t_d : Thickness of diaphragm
 σ_{du} : Tensile strength of diaphragm

Fig. 6 Analytical Model on ID Type



$$P_u = \min(P_c + P_s, P_w)$$

$$P_s = h_v \cdot t_v \left\{ (1 + \beta) \sigma_{sv} + (1 - \beta)(1 - \alpha) \sigma_{sv} \right\} \cos \theta$$

$$P_w = t \left[2h_r \cdot \sigma_{wu} + \frac{2(h_1 + h_2)}{3n^2} \left[\sigma_{sv} + \frac{n-1}{2} \left\{ (2n+1) \sigma_{sv} + (n+2) \sigma_{sv} \right\} \right] \right]$$

$$h_r = t_v + r_1 + r_2 + \kappa(h_1 - r_2) \quad h_1 = x \quad h_2 = x - \kappa(h_1 - r_2)$$

$$n = 1 + \frac{1}{\alpha} \left(\frac{\sigma_{wu}}{\sigma_{sv}} - 1 \right) \quad \beta = 0.9 - 0.05 \frac{h_v}{t_v} \quad \kappa = (1 + \beta)/2$$

P_c : Morita's yield line theory for ultimate out-of-plane resistance of steel tube's flange⁽²⁾
 t : Thickness of steel tube
 t_v : Thickness of stiffener
 x : Size of yield line theory⁽²⁾
 α : Reducing rate for second slope on bi-linear modeling of stress-strain curve
 θ : See Fig. 2
 σ_{sv}, σ_{wu} : Yield point of stiffener, tube web
 σ_{sv}, σ_{wu} : Tensile strength of stiffener, tube web

Fig. 7 Analytical Model on SV Type

which beam flanges were welded. In Fig. 4, load-displacement relation with different beam-column width ratio B/D is compared. Fig. 4 depicts that IL1 specimen with $B/D = 1/2$ shows 15 % higher yielding load and ultimate load than IL4 with $B/D = 1/3$. This comparison reveals that the beam width may affect load resistance of the diaphragm. Furthermore, the effects of steel tube's width-thickness ratio (IL1, IL5) and steel strength (IL1, IL6) were found to be minor on deformation capacity of local part of the connection.

Tensile test results for VS type are illustrated in Fig. 5. In these tensile tests, specimens failed by wearing of web steel at a corner of steel rectangular tube. Fig. 5 demonstrates that the specimen with high-rise stiffener (VL2) maintained greater load resistance than that with low-rise stiffener (VL1). The effect of steel width-thickness ratio (VL1, VL5) and steel strength (VL1, VL6) was also found to be minor.

3.2 Ultimate Strengths

A method is proposed to predict ultimate tensile load resistance of beam-column connection in this study. Calculation regimes in this method are represented in Fig. 6 for ID type and in Fig. 7 for VS type. In these regimes, ultimate resistance is calculated by superposing resistances of steel tube's flange and strengthening elements. This out-of-plane resistance of steel tube's flange is predicted by using so called yield line theory by Morita et al^{(1),(2)}.

Fig. 6 illustrates an analytical model in establishing formula for ID type, in which a diaphragm is assumed as diagonal braces. These braces are classified into two parts, A-part and B-part, according

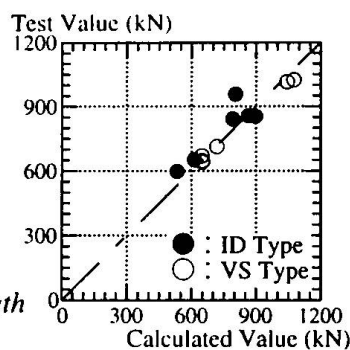


Fig. 8 Comparison in Ultimate Tensile Strength of Calculated Result and Test Result

to their resisting mechanism, in Fig. 6. This classification was adopted by analyzing the test results in which the load resistance was different depending on beam width. A-part is assumed to be directly transferred force by beams, and B-part is assumed to resist depending on the deformation of the steel tube.

Fig. 7 illustrates an analytical model for VS type, in which the stiffener is assumed as tension element with effective height. This effective height is determined by referring to the test results of strain distribution in stiffeners. By considering the fact that the failure occurred at the tube web in the tests, ultimate resistance is assumed as a smaller value of above mentioned superposition or tensile load capacity of the tube web. The prediction results using these calculation regimes were consistent with the test results. This agreement is demonstrated by the ratio of test result to the prediction result (agreement index), which is from 0.95 to 1.12 for ID type and from 0.95 to 1.04 for VS type (Fig. 8).

4 Structural Characteristics of the connection panels

4.1 Test Results

Shear test results are represented in Fig. 9 for ID type and Fig. 10 for VS type. All specimens maintained shear resistance up to 0.04 rad., and showed similar shear deformation ability independent of steel tube's width-thickness ratio, and steel strength. Shear resistance was higher for smaller height-width ratio of the connection panel. This tendency may be attributed to the difference of arch mechanism on filled concrete due to this ratio.

4.2 Ultimate Strengths

Calculated ultimate shear capacity is very conservative using the conventional formula in design guideline⁽³⁾ for steel reinforced concrete structures. This tendency is demonstrated using agreement index, which is in range from 1.30 to 1.48 for this case (Fig. 12). Therefore, the authors proposed

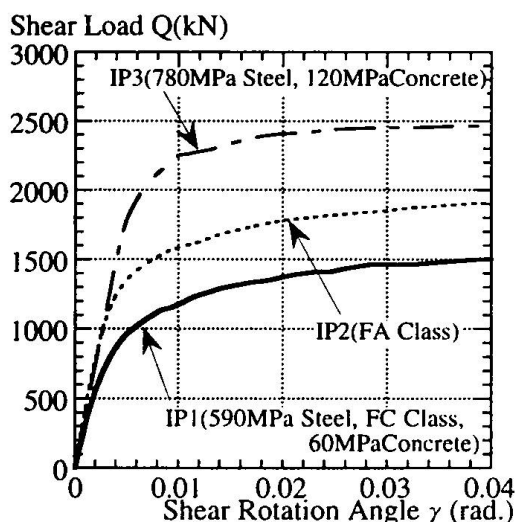


Fig. 9 Shear Tests Result on ID Type

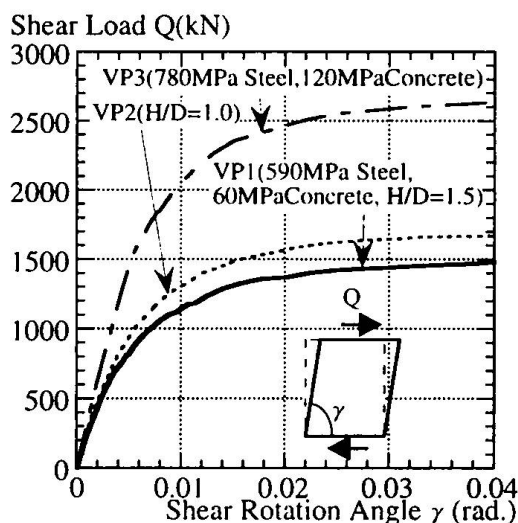


Fig. 10 Shear Tests Result on VS Type

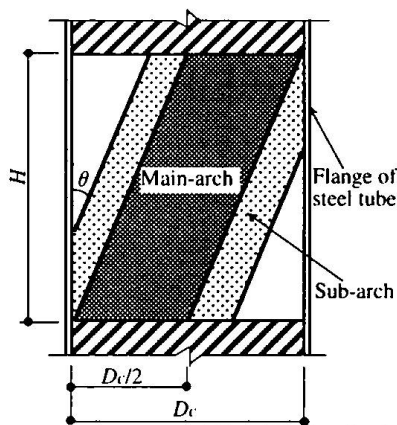


Fig. 11 Analytical Model on Connection Panel

$$Q_u = Q_s + Q_c$$

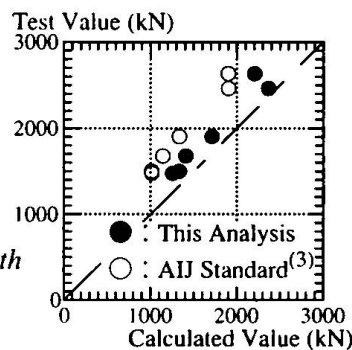
$$Q_s = A_w \cdot \frac{\sigma_{wu}}{\sqrt{3}}$$

$$Q_c = \left(\frac{D_c}{2} + \frac{2}{\cos \theta} \sqrt{\frac{2M_p}{t_c \cdot \sigma_R}} \right) t_c \cdot \sigma_R \cdot \tan \theta$$

$$\theta = \tan^{-1} \left\{ \sqrt{1 + \left(\frac{H}{D_c} \right)^2} - \frac{H}{D_c} \right\}$$

A_w : Section area of steel tube's web
 M_p : Full plastic moment of steel tube's flange
 t_c : Thickness of filled concrete
 σ_R : Compressive strength of filled concrete
 σ_{wu} : Tensile strength of steel tube's web

Fig. 12 Comparison in Ultimate Shear Strength of Calculated Result and Test Result



new design regime to predict ultimate shear resistance (Fig. 11). These factors have been developed under assumption that the shear resistance can be predicted by superposing the resistance of concrete and steel tube. The resistance of concrete is evaluated using arch mechanism, and that of steel is also evaluated considering only the pure shear. Two types of arch are considered, main arch by concrete itself and sub-arch by confined effect of steel tube on concrete. The contribution of the sub-arch to shear resistance was assumed to be the same as the flexural resistance of tube flange, which is calculated by assuming this flange as a cantilever. The agreement index for this regime ranged from 1.11 to 1.20 thus demonstrating good agreement between test and prediction results (Fig. 12).

5 Conclusion

- Deformation capacity of beam-column connection was little affected by the steel tube's width-thickness ratio, steel strength (590, 780MPa), or concrete strength (60, 120MPa).
- Ultimate tensile resistance of beam-column connection was successfully evaluated by superposing out-of-plane resistance of steel tube's flange and tensile resistance of local strengthening elements, which are assumed as simple tensile elements.
- Ultimate shear resistance of beam-column connection was successfully evaluated using superposition of steel tube's shear resistance and concrete shear resistance, which is calculated based on arch mechanism.

References

- Koji Morita, Masaru Teraoka, Takahiko Suzuki : Experimental Study on Connections Between Concrete Filled Square Tubular High Strength (780N/mm²) Steel Column and H-Beam, Proceedings of Third Pacific Structural Steel Conference, pp.591-598, 1992.8
- Noboru Yamamoto, Koji Morita, Hitoshi Watanabe : Effect of Stiffener on the Strength of Connection Between Beam and RHS Column, Proceedings of the Third International Symposium, Elsevier Applied Science, pp.172-179, 1990
- Architectural Institute of Japan : Standards for Structural Calculation of Steel Reinforced Concrete Structures, Architectural Institute of Japan, pp.44-46, 1991.9.20